CO2MVS RESEARCH ON SUPPLEMENTARY OBSERVATIONS

D2.4 Analysis of ratios of atmospheric columns over and downwind of emission hotspots located in contrasting geographical regions and the responsible ratios of emitted trace gases.

Due date of deliverable	December, 2024
Submission date	December 2024
File Name	CORSO-D2-4-V2.0
Work Package /Task	WP2/Task 2.4
Organisation Responsible of Deliverable	UEDIN
Author name(s)	Chlöe Schooling, Paul Palmer
Revision number	2
Status	Issued
Dissemination Level / location	Public

The CORSO project (grant agreement No 101082194) is funded by the European Union.

1 Executive Summary

This work has been done as part of WP2, which focuses on the use of co-emitted species to better estimate anthropogenic emissions in the future CO2MVS capacity. The main aim of this study was to assess the possibility of inferring emission ratios of $CO:CO_2$ and $NO_x:CO_2$ from satellite column observations of $CO:CO_2$ and $NO_2:CO_2$.

To achieve this, we analysed the output from the GEOS-Chem atmospheric chemistry 3-D model over mainland Europe for January and July 2021. We assessed the correlation between the emission ratios of $CO:CO_2$ and $NO_x:CO_2$, with the corresponding column enhancement ratios $\Delta CO:\Delta CO$ and $\Delta NO_2:\Delta CO_2$ downwind of emission sources. Overall, we find a very weak positive correlation for the respective CO ratios (R=0.12 January, R=0.10 July), and a very weak negative correlation was found for the respective NO_2/NO_x ratios (R=-0.14 January, R=-0.20 July).

To conclude, the weakness of these correlations reflects limited utility for deriving a reliable estimate for emission ratios from the observed column ratios for both pairs of species. Therefore, we suggest that a more sophisticated analysis to infer the emission ratios using a modelling inversion approach will be necessary going forwards. This will be explored in D2.7.

Table of Contents

2 Introduction

2.1 Background

To enable the European Union (EU) to move towards a low-carbon economy and implement its commitments under the Paris Agreement, a binding target was set to cut emissions in the EU by at least 40% below 1990 levels by 2030. European Commission (EC) President von der Leyen committed to deepen this target to at least 55% reduction by 2030. This was further consolidated with the release of the Commission's European Green Deal on the 11th of December 2019, setting the targets for the European environment, economy, and society to reach zero net emissions of greenhouse gases in 2050, outlining all needed technological and societal transformations that are aiming at combining prosperity and sustainability. To support EU countries in achieving the targets, the EU and European Commission (EC) recognised the need for an objective way to monitor anthropogenic CO_2 emissions and their evolution over time.

Such a monitoring capacity will deliver consistent and reliable information to support informed policy- and decision-making processes, both at national and European level. To maintain independence in this domain, it is seen as critical that the EU establishes an observation-based operational anthropogenic CO_2 emissions Monitoring and Verification Support (MVS) (CO2MVS) capacity as part of its Copernicus Earth Observation programme.

The CORSO research and innovation project will build on and complement the work of previous projects such as CHE (the CO_2 Human Emissions), and CoCO2 (Copernicus CO_2 service) projects, both led by ECMWF. These projects have already started the ramping-up of the CO2MVS prototype systems, so it can be implemented within the Copernicus Atmosphere Monitoring Service (CAMS) with the aim to be operational by 2026. The CORSO project will further support establishing the new CO2MVS addressing specific research & development questions.

The main objectives of CORSO are to deliver further research activities and outcomes with a focus on the use of supplementary observations, e.g., co-emitted species or auxiliary observations to better separate fossil fuel emissions from the other sources of atmospheric CO_2. CORSO will deliver improved estimates of emission factors/ratios and their uncertainties as well as the capabilities at global and local scale to optimally use observations of co-emitted species to better estimate anthropogenic CO_2 emissions. More broadly, CORSO will also provide clear recommendations to CAMS, ICOS, and WMO about the potential added-value of high-temporal resolution $^{14}CO_2$ (radiocarbon) and APO (atmospheric potential oxygen) observations as tracers for anthropogenic emissions in both global and regional scale inversions and develop coupled land-atmosphere data assimilation in the global CO2MVS system constraining carbon cycle variables with satellite observations of soil moisture, LAI (leaf area index), SIF (solar induced fluorescence), and biomass. Finally, CORSO will provide specific recommendations for the topics above for the operational implementation of the CO2MVS within the Copernicus programme.

2.2 Scope of WP2

The work presented in this report is part of WP2 of CORSO, which deals with “Use of co-emitted species (correlations, improved emission ratios, uncertainties) in data assimilation systems”. The aim of WP2 is to improve the use of observations of co-emitted species (NO_2, CO) to better estimate anthropogenic CO_2 emissions in the future CO2MVS capacity. This is based on the recognition that anthropogenic CO_2 emission estimates cannot generally be constrained using CO_2 concentration observations alone, and the detectability of the anthropogenic signal of co-emitted species, typically with much shorter atmospheric lifetimes, is often much better than that of CO_2. For the emission estimation development at local scale, this WP focuses on the development of methods to increase the accuracy of annual CO_2

emission estimates of hot spots, industrial and urban areas by integrating satellite observations of co-emitted species (NO_2 and CO) in data assimilation systems. Since CO_2 satellite observations are temporally sparse (even with the future CO2M constellation), temporal sampling biases are a significant source of uncertainty in annual CO_2 emission estimates of hot spots. Co-emitted species such as CO and NO_2 are and will be available at sub-diurnal temporal coverage from current and future LEO and GEO satellites. They can therefore be used to improve the constraint on the temporal variability of CO_2 emissions and hence for reducing the uncertainty in annual CO_2 emission estimates. The local and regional studies will focus on three regions: Europe, Africa, and Southeast Asia.

2.2.1 Scope of this deliverables

The estimation of CO_2 emissions from the observation of co-emitted species such as CO or NO_2 requires accurate knowledge of both the emission ratios ($CO:CO_2$ and $NO_x:CO_2$) and the corresponding atmospheric column ratios ($CO:CO_2$ and $NO_2:CO_2$ ratio in the atmospheric column. In this task, we use an atmospheric chemistry transport model to understand the relationship between emission ratios of CO_2:NO_x:CO and the corresponding atmospheric (column) ratios of CO_2:NO_2:CO. This complements the national scale analysis in VERIFY and the plume studies in CoCO2.
In this deliverable, we use modelled satellite column data to replicate OCO-2 CO_2 columns and TROPOMI NO_2 and CO columns. We explore the relationship between the input emission ratios with the observed column ratios downwind of emission sources through a simple correlation analysis. We do this to determine if we can expect to observe a direct relationship between emission ratios and column ratios to aid in the estimation of $ffCO_2$ through the observation of co-emitted species.

2.2.2 Work performed in this deliverable

The following activities have been conducted to achieve the deliverable; they are presented in detail in Section 3:

- GEOS-Chem model runs for January and July 2021 with TNO emission inputs,
- Modelled satellite column retrieval for OCO-2 (CO_2) and TROPOMI (NO_2, CO),
- Column enhancements of a particular gas in relation to the background concentration are calculated by removing latitude dependent background concentration of each gas (ΔCO_2, ΔCO, ΔNO_2),
- Analysis of how the emission inventory ratios ($CO:CO_2$, $NO_x:CO_2$ correlate with the atmospheric column enhancement ratios downwind of the sources $\Delta NO_2:\Delta CO_2$, $\Delta CO:\Delta CO_2$).

2.2.3 Deviations and counter measures

There were no deviations from the original work plan.

2.3 Project partners

CORSO Partners / Collaborators /Laboratories	
EIDGENOSSISCHE MATERIALPRUFUNGS- UND FORSCHUNGSANSTALT	EMPA
EUROPEAN CENTRE FOR MEDIUM-RANGE WEATHER FORECASTS	ECMWF
KAMINSKI THOMAS HERBERT	iLab
NEDERLANDSE ORGANISATIE VOOR TOEGEPAST NATUURWETENSCHAPPELIJK ONDERZOEK	TNO
UNIVERSITY OF EDINBURGH	UEDIN
UNIVERSITE PAUL SABATIER TOULOUSE III	UT3
WAGENINGEN UNIVERSITY	WU

3 Data and methods

Here, we describe how we used the GEOS-Chem atmospheric transport model with TNO emission inputs to simulate satellite columns and assess the relationship between emission ratios ($CO:CO_2$, $NO_x:CO_2$) and the corresponding enhanced column ratios ($CO:CO_2$, $NO_2:CO_2$) downwind of emission sources.

Our analysis follows on from a previous study (Sadiq et al., 2021) that analysed model and satellite data for the year 2018 on a country-level basis within mainland Europe. This study determined the Pearson correlation coefficient, and found a very weak positive correlation between the emission ratio and column enhancement ratio of $CO:CO_2$ (R=0.14), and a stronger negative correlation between the emission ratio $NO_x:CO_2$ and the column enhancement ratio of $NO_2:CO_2$ (R=-0.67). We follow a similar method to Sadiq et al., 2021, but this time focussing on the year 2021. In addition, we performed an assessment of the relationship between emission and column ratios specifically downwind from emission sources.

We opted to focus this study solely on modelled data, due to the limited amount of available data overlapping for CO_2, CO, and NO_2 measurements, from OCO-2 and TROPOMI. Using modelled satellite retrievals allowed us to undergo a direct analysis of how the influence of transport and chemistry translate emissions to observed columns in a perfect scenario (i.e. no data gaps in observations due to clouds or aerosol loading, and no instrument noise or retrieval errors). This approach provides a controlled framework for exploring any direct links between the emission ratios and the corresponding column ratios.

We present figures showing the spatial distribution of the modelled column enhancements, the emission sources, and the ratios of each for a single day in January and July (15th of the month), to give the reader a visual understanding of of how emissions translate into observed column enhancements under different seasonal conditions. We then apply a correlation analysis to the simulated data for every day in each of these months.

3.1 The GEOS-Chem Atmospheric Chemistry Transport Model

We use version 14.2.2 of the GEOS-Chem atmospheric chemistry transport model to describe the emissions, transport, and chemical production/loss of atmospheric NO_x. For our study, we use a nested version of the full chemistry model, centred over mainland Europe (32.75 to 61.25° N, -15 to 40 ° E) with 47 vertical levels, approximately 30 of which are below the dynamic tropopause. The nested model runs with a horizontal spatial resolution of 0.25°x0.3125°, providing fine-scale insights into regional atmospheric processes. The initial conditions and lateral boundary conditions to the nested domain were created from a consistent global version of the GEOS-Chem model run, which was run at a coarser resolution of 4°×5°, with three-hourly output fields. The nested model's transport processes are simulated with a 5-minute timestep, while the chemical reactions are computed every 10 minutes. These finer timesteps are necessary to accurately resolve the fast dynamics of atmospheric transport and chemistry within the high-resolution domain. The model is driven by offline meteorology fields from the GEOS Forward Processing (GEOS-FP) product from the Global Modelling and Assimilation Office (GMAO) at NASA Goddard Space Flight Center. GEOS-FP has a native horizontal resolution of 0.25°x0.3125° with 72 vertical pressure levels and 3 hr temporal resolution. To reconcile the 3-hourly meteorological input from the GEOS-FP dataset with the shorter model timesteps, the meteorological fields are linearly interpolated in time. By combining high-resolution meteorology with short timesteps for transport and chemistry, the

nested GEOS-Chem model achieves a detailed and realistic representation of atmospheric processes in the study domain.

The full-chemistry model was used to simulate the atmospheric transport, dispersion, and chemical reactions of CO and NO_x, where we resolve the CO and NO_2 tropospheric columns for a given set of prescribed emissions. However, CO_2 is not included in GEOS-Chem full-chemistry. Therefore, to model CO_2 emissions and relative concentrations we used the GEOS-Chem carbon model. The production of CO_2 from the oxidation of CO is calculated offline in the carbon model and added to the total CO_2 burden independently of the primary CO_2 emissions from direct sources. These primary CO_2 emissions are derived from emission inventories, while the secondary CO_2 contribution from CO oxidation is calculated using the output of the full-chemistry simulation. Due to the limited chemical interactions of CO_2 with any other atmospheric species, the outputs from the full-chemistry and carbon model runs can be analysed together without introducing significant inconsistencies. This separation allows for accurate representation of CO_2 levels while ensuring that chemical processes involving CO and NO_x are fully captured in the primary simulation.

The model was run for January and July 2021, and the species concentrations were output at a temporal resolution of 10 minutes. To determine modelled satellite data we extract the columns at 13:30 LST to the nearest 10 minutes, corresponding the local equatorial crossing time of the OCO-2 and TROPOMI satellites, described below.

3.1.1 Emission inventory

We used the TNO (Nederlandse Organisatie voor Toegepast Natuur- wetenschappelijk Onderzoek; Netherlands Organisation for Applied Scientific Research) GHGco v5.0 emission inventory at 0.1° × 0.05° resolution (Super et al., 2020). We apply scaling factors provided by TNO to reflect monthly, hourly, and daily patterns in emissions by sector.

TNO category	Sector	Combustion Type
A	Public Power	Combustion
B	Industry	Combustion
C	Other Stationary Combustion	Combustion
D	Fugitives	Non-Combustion
F	Road	Combustion
G	Shipping	Combustion
H	Aviation	Combustion
I	Off-road	Combustion
Z	Non-combustion	Non-Combustion

Table 1. TNO emission sector categories

The TNO categories by sector are shown in Table 1, where both combustion and non-combustion sources are included. We identified emission hotspots as regions with emissions exceeding the 99.5th percentile of emissions of the given species for the calculated for each month.

Note that while we are resolving NO_2 columns, in line with available observation data (TROPOMI), we must input the combined emissions of NO and NO_2 (NO_x), since NO rapidly converts to NO_2 in the atmosphere and therefore NO emissions will directly contribute to the observed NO_2 column value.

3.2 Modelling satellite columns and calculating column enhancements

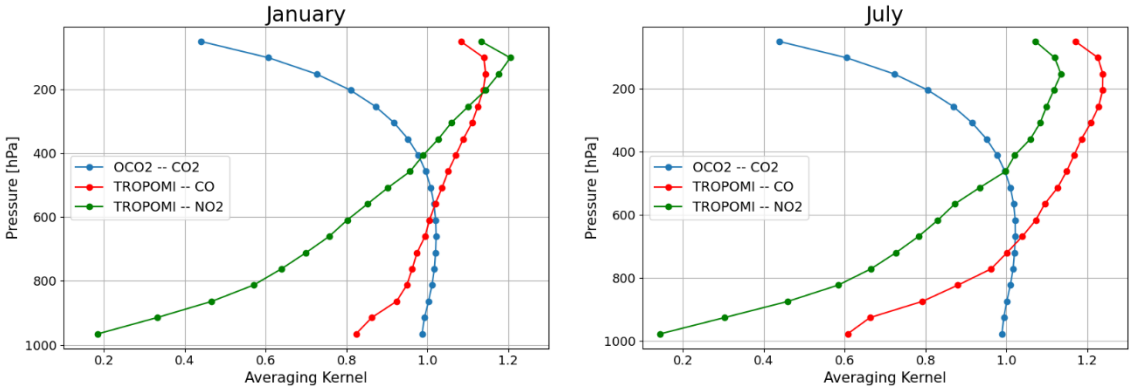

Figure 1: Median averaging kernels from the OCO-2 retrieval of CO_2 and the TROPOMI retrievals of CO, NO_2 for January and July. OCO-2 averaging kernels were obtained from the ACOS OCO-2 Level 2 data, version 10, and the TROPOMI averaging kernels were obtained from the S5P Level 2, product version 2.2.0, processing version 1.6.0.

We simulated satellite columns of CO_2 from OCO-2 (Orbiting Carbon Observatory-2), and NO_2 and CO from TROPOMI (TROPOspheric Monitoring Instrument). Both satellites follow a sun-synchronous orbit with a local equatorial crossing time of 13:30. To model realistic data we applied the monthly median averaging kernels for each gas (from OCO-2 and TROPOMI) to account for the varying sensitivity to these gases through the atmosphere. These averaging kernels are shown in Fig.1 1. OCO-2 generally have more sensitivity to changes in CO_2 in the lower atmosphere. Conversely, TROPOMI is typically less sensitive to changes in NO_2 and CO at lower altitudes.

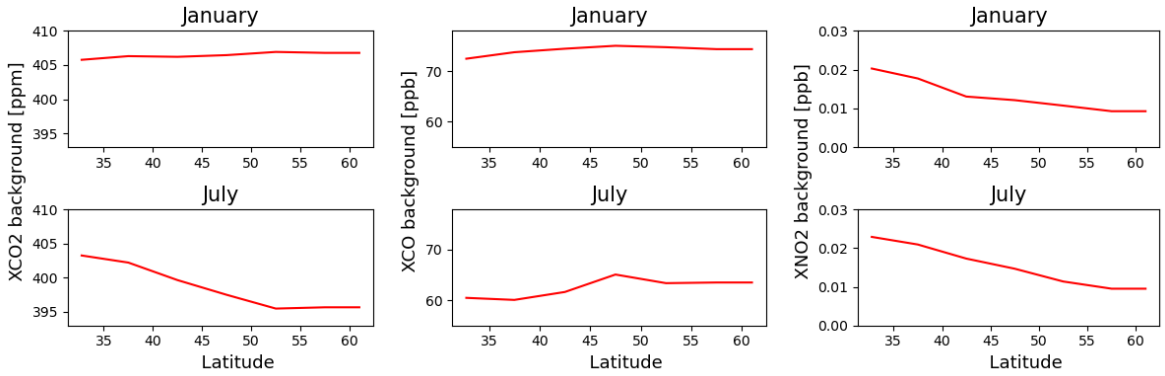

Figure 2: Background levels as a function of latitude for the tropospheric columns of CO_2, CO, NO_2 for January and July.

We convert the tropospheric columns (XCO_2, XCO, XNO_2), to column enhancements (ΔCO_2, ΔCO, ΔNO_2) by removing the monthly averaged background levels for each gas (i.e. not influenced by emission enhancements). We do this to isolate the influence of recent emissions. The background was determined as the 1st percentile value of the tropospheric column over mainland Europe (32.75 to 61.25° N, -15 to 40 ° E) across each month of data. We calculated this as a function of latitude using 5° latitude bins. We used 5° latitude bins to balance capturing latitudinal variability in background gas levels with minimizing noise from localized model fluctuations or small-scale variations. The background levels for the three gases, in January and July are shown in Fig. 2.

4 Results and discussion

4.1 The emission inventory and emission ratios NO_x:CO_2 and CO:CO_2

The spatial distribution of the emissions of CO_2, CO and NO_x are shown in Fig. 3 at 13:00 GMT for a single day (15th of the month) in January and July. There are obvious regions of elevated emissions, which we identify as emission sources. The spatial distribution of the emissions is very similar for the winter and summer months, but the magnitude of emissions is somewhat reduced in the summer. Diurnal, weekday and monthly scaling factors for each emission sector (Table 1) are applied to the emission sources to reflect the temporal changes in emissions. The mean CO_2 emission is 1.6×10^{-8} kg/m^2/s in January and 1.3×10^{-8} kg/m^2/s in July; the mean CO emission is 1.1×10^{-10} kg/m^2/s in January and in 6.3×10^{-11} kg/m^2/s July; and the mean NO_x emission is 7.0×10^{-10} kg/m^2/s in January and 9.3×10^{-10} kg/m^2/s in July.

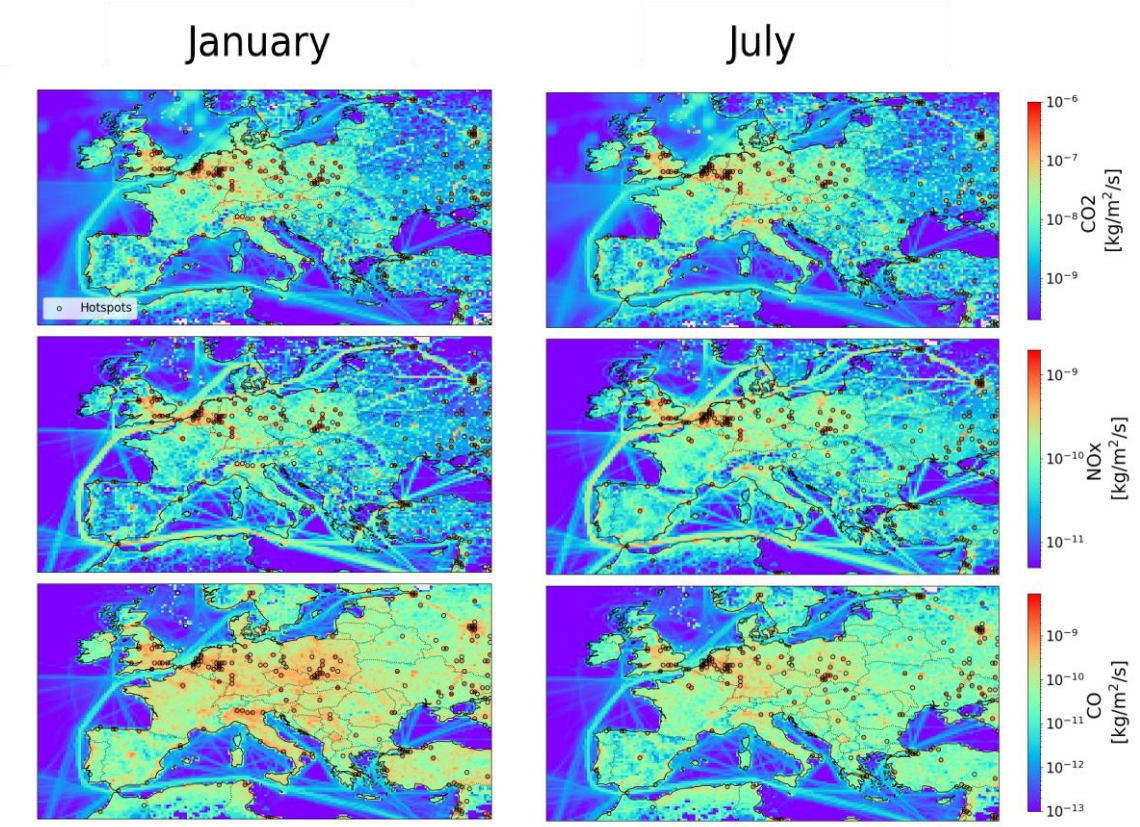

Figure 3: Spatial distribution of the TNO emission inventories of CO_2, CO, and NO_x at 13:00 on a single day in January and July. The identified emission hotspots (where emissions exceed 99.5th percentile) are highlighted with rings.

We then calculate the CO:CO_2 and NO_x:CO_2 emission ratios, described as mole fractions (Fig 4). These gridded ratios provide insight into the net combustion efficiency and characteristics of total emissions across sources. Higher CO:CO_2 ratios generally indicate lower combustion efficiency, as incomplete combustion produces more CO relative to fully oxidized CO_2. The NO_x:CO_2 ratio, while less directly tied to combustion efficiency, is influenced by combustion temperature, with higher ratios typically associated with elevated temperatures that promote NO_x formation. Additionally, the use of emission control technologies such as catalytic converters and filters can alter these ratios, often reducing NO_x emissions.

Our findings show that the CO:CO_2 ratios tend to be higher in January, while the NO_x:CO_2 ratio tends to be higher in July. In addition, we see a trend of higher ratios across the eastern

side of Europe. In general, the magnitude of these ratios tends to be reflected by the dominant emission sectors for different regions/seasons (Sadiq et al., 2021).

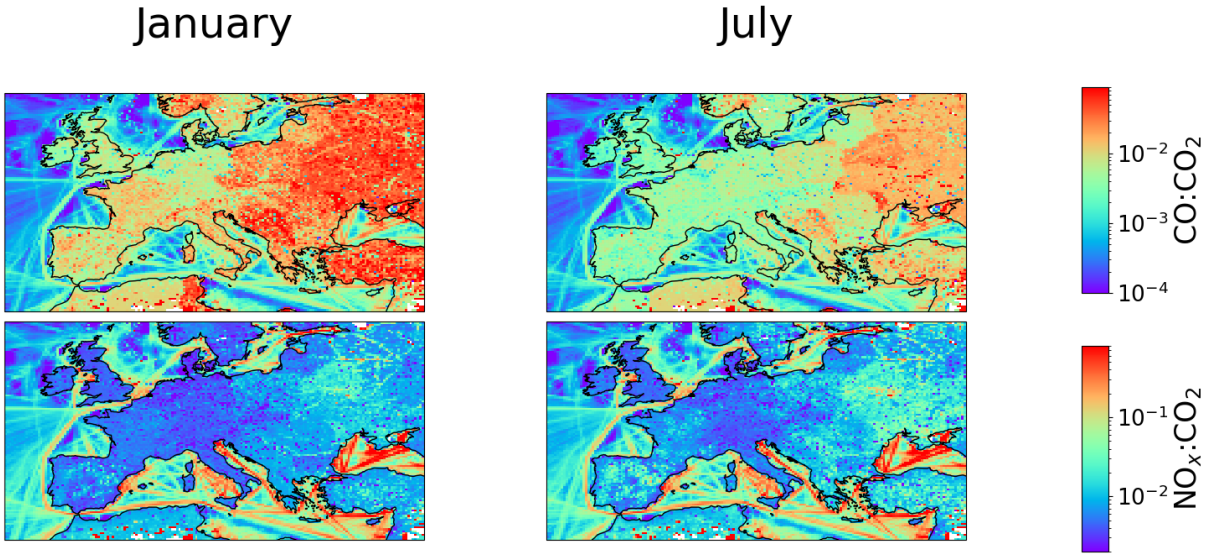

Figure 4: Spatial distribution of the emission inventory ratio CO:CO_2 and NOx:CO_2 for a day in January and a day in July.

4.2 Modelled satellite columns and corresponding enhanced column ratios ΔNO_2: ΔCO_2 and ΔCO: ΔCO_2

We use the GEOS-Chem model driven by emission inventories, to describe TROPOMI CO, NO_2, and OCO-2 CO_2. Fig. 5 shows the modelled satellite columns (retrieved at 13:30 overpass) and corresponding column enhancements for a day in January and July (15th of the month). As expected, we observe a strong seasonal decrease in the overall levels of CO_2 from January to July due to significant changes in vegetation. A similar, but less prominent trend is seen for CO and NO_2, which can be explained by increased photochemical activity and lower emission rates in the summer months. We observe distinct regions with pronounced peaks in column levels with a similar spatial distribution of elevated regions between the three gases for all days of the month.

The enhanced columns (ΔCO_2, ΔCO, ΔNO_2) are normalised so the minimum value is zero, where any regions with a value of zero are assumed to be presenting no influence from emissions. When comparing XCO_2 to ΔCO_2 we see some pronounced peaks appear that were not obvious before, especially in July, when the background CO_2 levels have higher dependence on latitude. The spatial distributions of ΔCO and ΔNO_2 are less significantly changed in comparison to the raw column values, reflected by the lower background levels of these species.

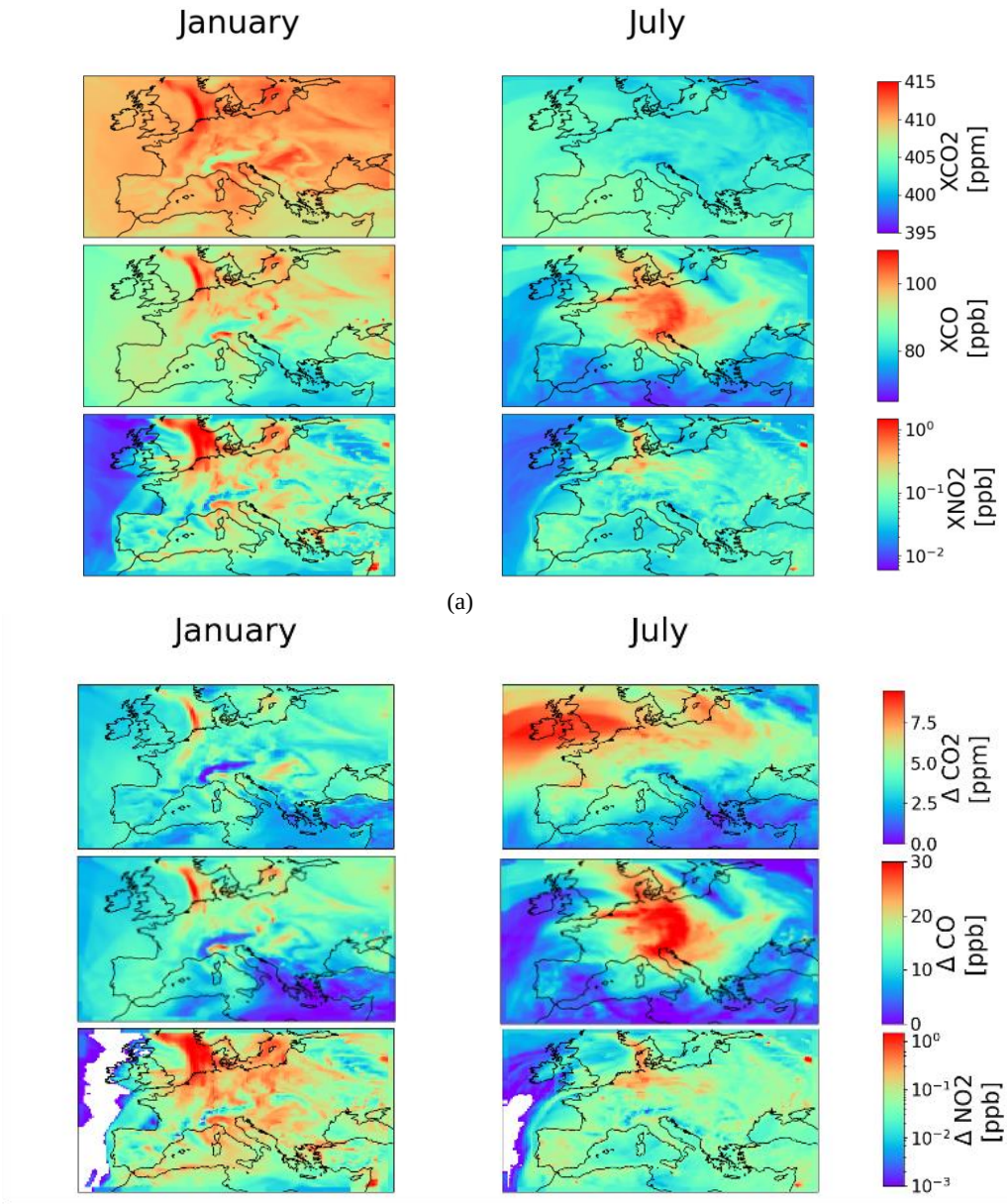

Figure 5: Spatial distribution of (a) the modelled satellite tropospheric columns and (b) the corresponding column enhancements after removing the latitude dependent background levels. Note due to the logarithmic scale that the white area in NO_2 enhancement plot, show value of zero for the column enhancement.

Using the enhanced columns, we calculate the column ratios $\Delta CO:\Delta CO_2$ and $\Delta NO_2:\Delta CO_2$ (Fig. 6). The ratio of $\Delta CO:\Delta CO_2$ is generally relatively stable with a mean of 0.003 in both seasons (i.e. around 300 times more moles of enhanced CO_2 than CO). There is more spatial variation in the inventory-based $CO:CO_2$ than the corresponding atmospheric enhancement ratio $\Delta CO:\Delta CO_2$, which is due to the atmospheric mixing of CO that has an e-folding lifetime larger than the transport time over Europe. Any regions with significantly higher ratio values are influenced by relatively small values of ΔCO_2 such as over the Alps, where we may expect reduced impact from urban emissions. The ratio of $\Delta NO_2:\Delta CO_2$ is much more varied spanning 4 orders of magnitude, this is more analogous to the range in emission ratios, which is due to the much shorter e-folding lifetime of NO_2. The regions of higher $\Delta NO_2:\Delta CO_2$ ratio tend to be influenced by peaks in the ΔNO_2 columns that are not observed in ΔCO_2.

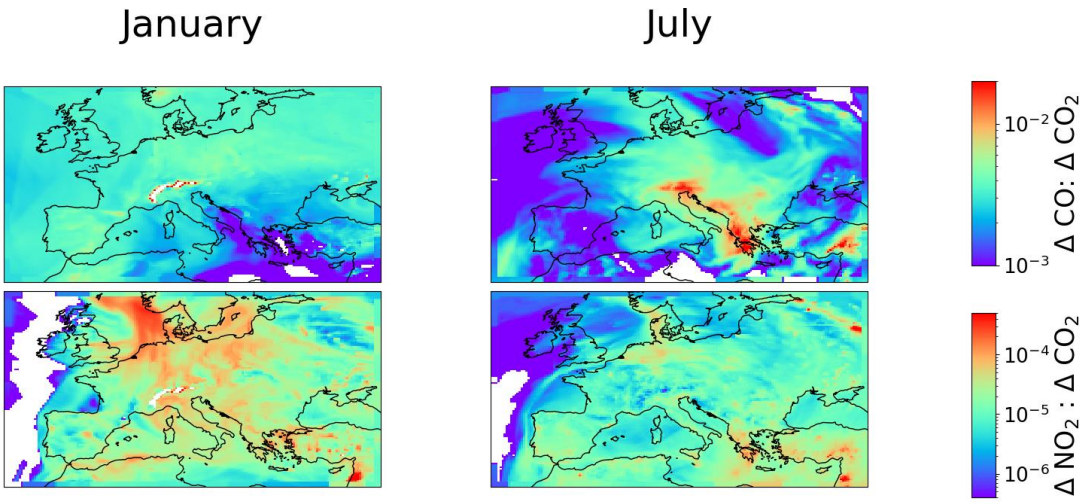

Figure 6: Spatial distribution of enhanced column ratios ΔCO:ΔCO$_2$ and ΔNO$_2$:ΔCO$_2$, for a day in January and a day in July.

4.3 Correlation between emissions and column ratios

Firstly, we performed a simple correlation analysis between the emission ratios and enhanced column ratios across all regions, linking the emissions at 13:30 to the corresponding column enhancement ratio in the same grid-point. The correlations are presented in Fig. 7, where we find insignificant correlation (R=0.0) for both months for the relationship between the inventory ratios of both CO:CO$_2$ and NO$_x$:CO$_2$ with their corresponding enhanced column ratio.

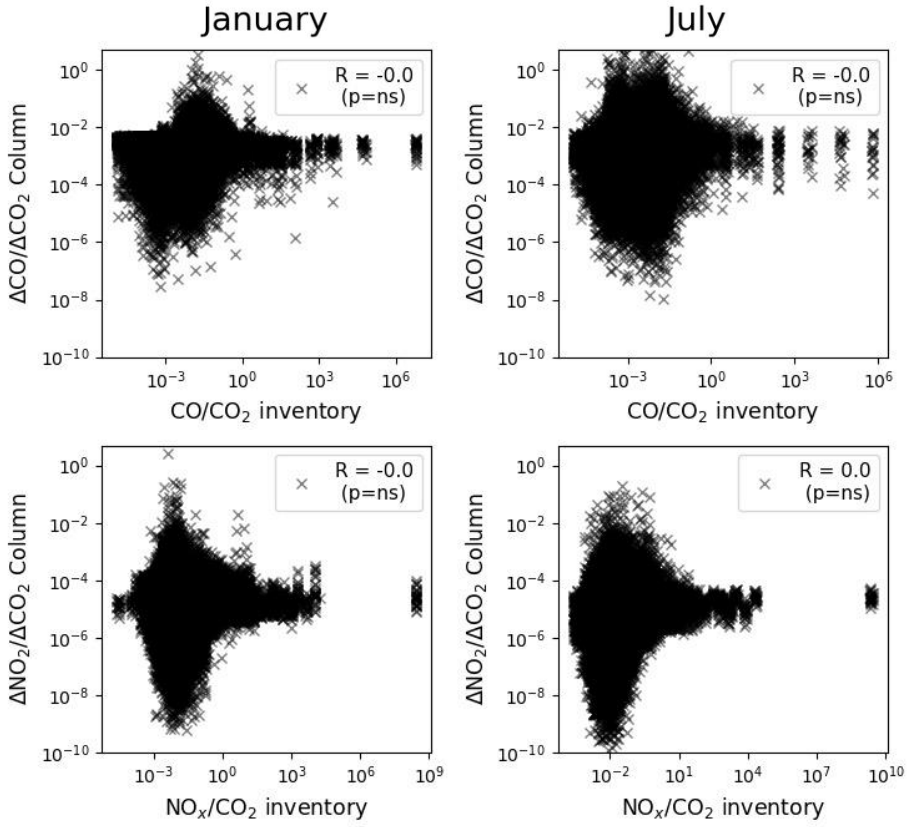

Figure 7: The relationship between the emission ratios CO/CO$_2$ and NO$_x$/CO$_2$ with each respective column enhancement ratios ΔCO:ΔCO and ΔNO$_2$:ΔCO$_2$ for a 13:30 retrieval over Europe for the whole month of January and July.

Since we are primarily interested in deriving emission ratios within sources, we design a more sophisticated analysis to assess this relationship in the columns downwind from emission hotspots. To analyse the columns downwind of emission sources, we identified all hotspots within 3 hours preceding the column retrieval at 13:30 local time. For each identified source, we located the corresponding column at 13:30 downwind of the source. To account for emission transport due to wind, we used the surface wind components (U, V) (in m/s), where U represents the east-west wind component, and V represents the north-south component. By multiplying the wind velocity by the time offset (in seconds), we calculated the displacement of the emission source. This displacement was then converted from distance to degrees, enabling us to pinpoint the grid cell corresponding to the downwind column. Finally, we performed a correlation analysis between the emission ratios in the sources and the enhanced column ratios at the identified downwind locations (Fig. 8).

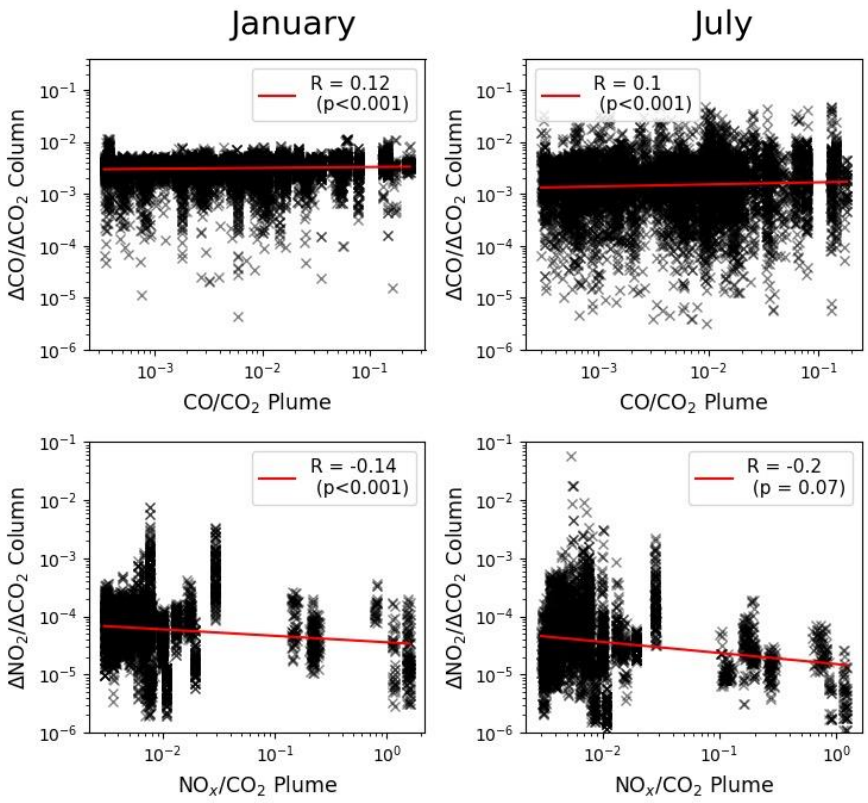

Figure 8: The relationship between the emission ratios CO/CO_2 and NO_x/CO_2 inside hotspot regions with each the column enhancement ratios $\Delta CO:\Delta CO$ and $\Delta NO_2:\Delta CO_2$ downwind of the source for a 13:30 retrieval over Europe for the whole month of January and July.

We found a generally very weak correlation between the emission ratios and corresponding column enhancement downwind of the source. The correlation is a very weak positive for the $CO:CO_2$ ratio relationship (R=0.12 January, R=0.10 July), and a very weak negative correlation for the $NO_x/NO_2:CO_2$ ratio relationship (R=-0.14 January, R=-0.20 July). This is a similar to the results determined by Sadiq et al., who performed a country-level analysis to determine the correlation between emissions and tropospheric column ratios evaluated for each individually country. Here we found weaker correlations by performing analysis on the individual emission sources, in comparison to the country-level analysis. The worsened correlation likely comes from the fact that a country-level analysis aggregates the emissions from multiple sources across the region and smooths out the effect of atmospheric dispersion, dilution, and mixing of the individual sources. However, to effectively use tracer gases to better

understand ffCO2 we need to be able to infer emission ratios for individual sources, not whole countries.

One consistency between our analysis and the study performed by Sadiq et al., is that while generally weak, we observe a positive relationship for CO:CO_2, and a marginally stronger negative relationship for NO_x:CO_2. Overall, this a reflection of CO chemistry being largely linear, where we see a proportional relationship between the amount of CO present and the rates of chemical reactions, but much more complex non-linear NO_x photochemistry, where we have strong non-linear effects of meteorological factors such as temperature and sunlight.

These correlations are likely to be very weak because both CO_2 and CO have relatively large e-folding lifetimes, and there will be a significant accumulation of atmospheric levels due to transport from a large spanning region and from a large period of time, which makes mapping the observation of a single column to a single emission hotspot very difficult. Overall, the weakness of these correlations reflects limited utility for deriving a reliable estimate for emission ratios from the observed column ratios for both pairs of species. From this we conclude that we need a more sophisticated approach to infer and understand our emission ratios using satellite data.

5 Conclusion

Overall, we found a limited relationship between emission ratios with the observation of column ratios downwind of the source. This suggests that it is not feasible to make a direct link from observed column ratios to a predicted emission ratio. In fact, in the case of the column ratio ΔNO_2:ΔCO_2 an observed increase in this ratio may be driven by a decrease in the respective NO_x:CO_2 emission ratio in the source.

The atmospheric observations of CO_2, CO, and NO_2 are subject to an intricate interplay of factors that complicate the direct derivation of emission ratios. These include atmospheric transport dynamics, such as advection and turbulent mixing, non-linear chemical reactions between species, as well as variations in background concentrations due to natural sources and sinks. Additionally, the e-folding lifetimes of these gases vary significantly: CO and CO_2 have relatively long atmospheric lifetimes compared to NO_2, meaning that for a given column observation, contributions arise from emissions over a broad spatial and temporal range. For example, the lifetime of CO_2 is far greater than the atmospheric transport time across Europe, leading to column concentrations that integrate emissions from diverse sources across wide geographic areas and timeframes.

Based on our finding, we suggest that the best route to determine emission ratios from satellite observations of CO_2 and the respective tracers would be using inverse modelling-based approach (e.g. Nayagam et al., 2023; Super et al., 2024). The data from VERIFY in sector-dependent emission ratios can be incorporated as priors in an inverse model, designed to minimise the difference in the observed and modelled column ratios of CO_2 and the respective tracers to improve our understanding of emission ratios. A combined CO:NO_x:CO_2 inversion model, can effectively account for atmospheric transport, chemical transformations, and spatiotemporal variability. Such methods to integrate satellite observations with model simulations to constrain emissions with greater accuracy will be explored in D2.7, using the NO_x chemistry framework developed in D2.5. By incorporating tracers such as CO and NO_x alongside CO_2, such models can provide more robust constraints on emission sources, ultimately leading to improved estimates of $ffCO_2$.

6 References

Balsamo, G., Engelen, R., Thiemert, D., Agusti-Panareda, A., Bousserez, N., Broquet, G., Brunner, D., Buchwitz, M., Chevallier, F., Choulga, M., et al.: The CO2 Human Emissions (CHE) Project: First steps towards a European operational capacity to monitor anthropogenic CO2 emissions, *Frontiers in Remote Sensing*, **2**, 707 247, 2021.

Jacob, D.: *Introduction to atmospheric chemistry*, Princeton University Press, Princeton, NJ, 1999.

Nayagam, L., Maksyutov, S., Oda, T., Janardanan, R., Trisolino, P., Zeng, J., Kaiser, J. W., and Matsunaga, T.: A top-down estimation of subnational CO2 budget using a global high-resolution inverse model with data from regional surface networks, *Environmental Research Letters*, **19**, 014031, https://doi.org/10.1088/1748-9326/ad0f74, 2023.

Sadiq, M., Palmer, P. I., Lunt, M. F., Feng, L., Super, I., Dellaert, S. N. C., & Denier van der Gon, H. A. C. (2021). Understanding the influence of combustion on atmospheric CO_2 over Europe by using satellite observations of CO_2 and reactive trace gases. *Atmospheric Chemistry and Physics Discussions*. https://doi.org/10.5194/acp-2021-816

Super, I., Dellaert, S. N., Visschedijk, A. J., and Denier van der Gon, H. A.: Uncertainty analysis of a European high-resolution emission inventory of CO2 and CO to support inverse modelling and network design, *Atmospheric Chemistry and Physics*, **20**, 1795–1816, 2020.

Super, I., Scarpelli, T., Droste, A., and Palmer, P. I.: Improved definition of prior uncertainties in CO2 and CO fossil fuel fluxes and its impact on multi-species inversion with GEOS-Chem (v12.5), *Geoscientific Model Development*, **17**, 7263–7284, https://doi.org/10.5194/gmd-17-7263-2024, 2024.

Document History

Version	Author(s)	Date	Changes
0.1	C. Schooling	November 29, 2024	
1.0		Dec 2024	
2.0	C. Schooling	Dec 17 2024	

Internal Review History

Internal Reviewers	Date	Comments
Marc Guevara, BSC and Jaroslaw Necki, AGH	Dec 2024	